Poly(dimethylsiloxane-*b*-styrene) Diblock Copolymers Prepared by Reversible Addition-Fragmentation Chain Transfer Polymerization: Kinetic Model

Cheng-Mei Guan, Zheng-Hong Luo, Pei-Ping Tang

Department of Chemical and Biochemical Engineering, College of Chemistry and Chemical Engineering, Xiamen University, Xiamen 361005, People's Republic of China

Received 5 June 2010; accepted 25 March 2011
DOI 10.1002/app.34570
Published online 9 August 2011 in Wiley Online Library (wileyonlinelibrary.com).

ABSTRACT: Well-defined polydimethylsiloxane-*block*-polystyrene (PDMS-*b*-PS) diblock copolymers were prepared by reversible addition-fragmentation chain transfer (RAFT) polymerization using a functional PDMS-macro RAFT agent. The RAFT polymerization kinetics was simulated by a mathematical model for the RAFT polymerization in a batch reactor based on the method of moments. The model described molecular weight, monomer conversion, and polydispersity index as a function of polymerization time. Good agreements in the polymerization kinetics were achieved for fitting the kinetic profiles with the developed model. In addition, the model was used to predict the effects of initiator concentration, chain transfer agent concentration, and monomer concentration on the RAFT polymerization kinetics. © 2011 Wiley Periodicals, Inc. J Appl Polym Sci 123: 1047–1055, 2012

Key words: PDMS-*b*-PS diblock copolymers; RAFT polymerization kinetics; mathematical modeling; polymerization engineering

INTRODUCTION

Poly(dimethylsiloxane-*b*-styrene) (PDMS-*b*-PS) combines the unique properties of silicone polymers with those of polystyrene (PS).[1–3] Association between these two polymers opens a way to various industrial applications. For instance, PDMS-*b*-PS copolymers can be used as thermoplastic elastomers, compatibilizers, and surfactants in polymer blends.[4–6] However, PDMS-*b*-PS copolymers have been achieved mainly by living polymerization techniques, such as living anionic polymerization,[7–9] group-transfer polymerization,[10] and living radical polymerization (LRP),[9,11] etc. Recently, much interest has been devoted to LRP, as it provides greater monomer diversity and less stringent reaction conditions specifically in regard to monomer purification.[12] Since the discovery of LRP by Otsu et al. in 1982,[13] a plethora of powerful LRP techniques have been developed, including but not limited to nitroxide-mediated LRP (NMP),[14] reversible addition/fragmentation transfer (RAFT) polymerization,[15] and atom transfer radical polymerization (ATRP),[9] etc. Among them, ATRP can be applied for preparing well-defined block copolymers due to its ability to control polymer architecture, molecular weight and molar mass distribution, moderate experimental condition, etc.[9,11] With ATRP, the halide species is usually toxic and the catalyst complex used is easily oxidized in air. NMP technique also has restrictions of monomer choice and tends to operate at elevated temperatures.[16] The RAFT polymerization technique, however, is applicable to a wide range of monomers and can be applied to high conversion bulk polymerizations.[17–19] Furthermore, till now, no detailed research has been done using the RAFT polymerization technique to prepare the PDMS-*b*-PS copolymers. Accordingly, it is desirable to develop a novel approach to synthesize directly PDMS-*b*-PS copolymers.

However, recently, a series of PDMS-*b*-PS diblock copolymers were prepared by RAFT polymerization of styrene (St) using a PDMS-macro RAFT agent in our group.[20] The results showed that PDMS-*b*-PS diblock copolymers with well-defined structures were successfully synthesized via the RAFT polymerization. The copolymer molecular weights measured by ^{1}H-NMR and GPC are close to those as predicted, and therefore we can confirm that the polymerization proceeded in a controlled manner. It provides an applicable approach to the preparation of PDMS-containing block copolymers using a

Correspondence to: Z.-H. Luo (luozh@xmu.edu.cn).

Contract grant sponsor: The National Natural Science Foundation, China; contract grant numbers: 20406016, 21076171.

Contract grant sponsor: Nation Defense Key Laboratory of Ocean Corrosion and Anticorrosion, China; contract grant number: 51449020205QT8703.

Contract grant sponsor: Fujian Province Science and Technology Office, China; contract grant number: 2005H040.

© 2011 Wiley Periodicals, Inc.

PDMS-macro RAFT agent with a xanthate group. However, the RAFT polymerization kinetics of St was not investigated in our previous work.[20] In addition, the effects of polymerization conditions, such as initiator concentration and feed composition, etc. on the RAFT polymerization kinetics were still not investigated in our previous work.[20] In practice, the polymerization kinetics is an important proportion of polymerization engineering, which describes the changes of polymerization activity and polymer properties dependent on polymerization time.[21,22] Furthermore, the polymerization kinetics can be described using some model equations.

Till now, several open articles[23–32] have been published concerning the kinetic modeling of RAFT polymerization processes. Luo and coworkers[23,24,26] simulated the controlled/living radical copolymerization (CLRcoP) operated in a batch process to avoid composition drifting and thus produce spontaneous gradient copolymer. The control is based on a semibatch reactor technology with programmed comonomer feeding rates. Prior to this model, Luo and coworkers obtained the kinetics of the CLRcoP. However, Luo and coworkers RAFT polymerization process is not a RAFT polymerization process using a functional macromolecule RAFT agent and is operated at a semibatch way instead of a batch way. Smulders et al.[25,27,31] studied the continuous RAFT miniemulsion block copolymerization of St and *n*-butyl acrylate (BA) in a train of continuous stirred tank reactors (CSTRs). The reactor model was also developed in their works.[25,27,31] Soriano-Moro et al.[28] simulated the recently proposed dithiolactone-mediated radical polymerization of St. The RAFT-like dithio-compound controller behaves as a NMRP controller by presenting only reversible addition. The simulations based on the proposed reaction mechanism reproduce reasonably well the observed experimental data, although the model predicts a more controlled system. Altarawneh et al.[29] developed a mathematical model to account for the evolution of polymer product attributes in the emulsion RAFT polymerization of St. The effects of transfer agent, surfactant, initiator, and temperature were investigated. In addition, in Ref. 30 the molecular weight distribution formed in an ideal RAFT-mediated radical polymerization was considered theoretically. In this polymerization, the addition to the RAFT agent is reversible, and the active period on the same chain could be repeated, via the two-armed intermediate, with probability 1/2. Zhang and Ray[32] developed a mathematical model by combining living RAFT polymerization chemistry with a tank reactor model to analyze process development and design issues. Experimental data from MMA solution polymerization in a batch reactor were compared with the model to estimate the reversible reaction rate constants in the presence of the RAFT agent. Although interest in the RAFT polymerization is great, it still appears to be no models reported in the open literature at present to address the modeling of the RAFT process of St using a functional PDMS-macro RAFT agent to prepare PDMS-*b*-PS diblock copolymers. In addition, no studies have been reported that consider the influence of polymerization condition choice on RAFT polymerization of St using a functional PDMS-macro RAFT agent. Therefore, in this work, the RAFT polymerization kinetics is simulated by a mathematical model for the RAFT polymerization in a batch reactor based on the method of moments.

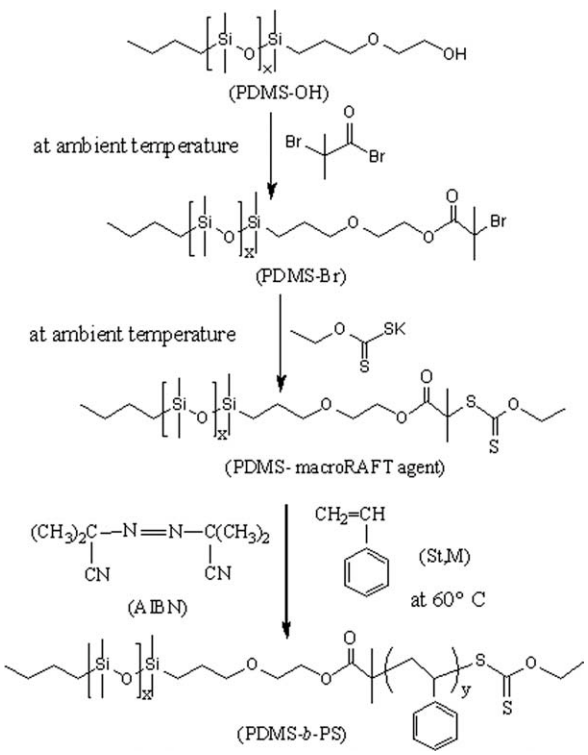

Scheme 1 Synthetic schemes of the PDMS-macro RAFT agent and the PDMS-*b*-PS diblock copolymers.

EXPERIMENTAL

The experimental section in this work is close to that reported in our previous work.[20] However, herein, the experimental section was still described in brief to keep the study complete.

Syntheses of the PDMS-*b*-PS diblock copolymers

Syntheses of the PDMS-*b*-PS diblock copolymers were described previously.[20] The PDMS-*b*-PS diblock copolymers were prepared by the RAFT polymerization of St (i.e., M) from dithioester group end-capped PDMS (PDMS-macro RAFT agent, I; see Scheme 1). As shown in Scheme 1, PDMS-macro RAFT agent was prepared from bromine end-capped PDMS (PDMS-Br) and PDMS-Br was obtained via

the esterification reaction of 2-bromoisobutyrylbromide with a commercially available PDMS-OH.

The RAFT polymerization was carried out in a dry flask under the inert atmosphere of nitrogen. The typical RAFT polymerization of St was using AIBN as initiator. AIBN (I) and PDMS-macro RAFT agent (T) were charged into a dry two-neck flask with a magnetic stirrer bar. Vacuum was then applied and the flask was flushed with nitrogen, which was run for three times. St and toluene were added in the flask using degassed syringes. The solution was flushed with nitrogen as described above, and was heated to 60°C by an oil bath. Samples were taken periodically with a syringe. The reaction was stopped after 5 h. In addition, the reaction mixtures were diluted with tetrahydrofuran (THF) and precipitated in methanol. The obtained polymer was rinsed with methanol for several times and dried to constant weight under vacuum at 50°C. Concerning the syntheses and characterizations of PDMS-*b*-PS diblock copolymers, readers are encouraged to refer to our previous work.[20]

Measurements

As described above, samples were taken periodically with a syringe and were dried to constant weight in vacuum at 50°C. The monomer conversion was measured by gravimetry of the above samples with constant weight. Therefore, the monomer conversions were recorded as a function of time and the polymerization rates were calculated by further differentiation. Besides, Fourier transform infrared (FTIR) spectra were recorded from KBr pellets on a Nicolet Avatar 360 FTIR spectrophotometer. The polymer samples were measured by nuclear magnetic resonance (^{1}H-NMR) on a Bruker AV400 NMR spectrometer in deuterated chloroform. The molecular weight (M_n) and molecular weight distribution (M_w/M_n, PDI) of the polymers sampled were determined at 40°C by gel permeation chromatography GPC. GPC was carried out using THF at a flow rate of 1 mL/min, with a Waters 1515 isocratic HPLC pump equipped with a Waters 2414 refractive index detector and three Waters Styragel HR columns (1×10^4, 1×10^3, and 500 Å pore sizes). Monodisperse PS standards were used for calibration.

Kinetic modeling of the RAFT process

Polymerization scheme

The RAFT polymerization process of St involves both conventional free radical polymerization kinetics and a RAFT reaction step in the presence of a RAFT agent. Different from ordinary RAFT polymerization processes, the RAFT polymerization process of St reported in this work[20] uses PDMS-macro RAFT agent as a RAFT agent. However, the polymerization scheme is still similar to that of the ordinary RAFT processes.[23–27,33] Therefore, referring to Refs. 23–27,33, the following polymerization scheme is applied:

$$I \xrightarrow{f,k_d} 2P_0^\bullet \tag{1}$$

$$P_r^\bullet + M \xrightarrow{k_p} P_{r+1}^\bullet \qquad r = 0,1,2,\ldots \tag{2}$$

$$P_r^\bullet + TP_s \xrightarrow{k_a} P_r\dot{T}P_s \xrightarrow{k_f} TP_r + P_s^\bullet \tag{3}$$

$$P_r^\bullet + P_s^\bullet \xrightarrow{k_{td}} P_r + P_s \tag{4}$$

$$P_r^\bullet + P_s^\bullet \xrightarrow{k_{tc}} P_{r+s} \tag{5}$$

$$P_r\dot{T}P_s + P_t^\bullet \xrightarrow{k_{ct}} P_{r+s+t} \tag{6}$$

where, I is the initiator (AIBN), $P_r\dot{T}P_s$ is the intermediate radical chain, TP_r is the dormant chain, $P_r^\bullet$ is the propagating radical chain, M is the monomer (St), and P_r and P_s are both the dead chain. In addition, eq. (1) is the chain initiation with k_d as the rate constant and f as the initiator efficiency due to cage effect. The number of 2 in eq. (1) accounts for the fact that one initiator molecule normally generates two radicals. eq. (2) is the chain propagation with k_p as the chain propagation rate constant. The subscript r represents the number of monomeric units that have been incorporated into chain. In addition, one knows that the value of the rate constant for the above each step is independent on chain length. eq. (3) is the addition and fragmentation reactions. T represents the chain-transfer-agent unit; k_a and k_f are the addition and fragmentation rate constants, respectively. Equations (4)–(6) are the bimolecular radical termination by disproportionation (k_{td}), combination (k_{tc}) and cross-combination (k_{ct}).

Defining chain moments and deriving moment equations

We use the method of moments.[26,33] There are four types of chain species involved in the RAFT polymerization system, namely, $P_r^\bullet$, $P_r\dot{T}P_s$, TP_r, and P_r. Their moments are defined in Appendix A. However, for the species including the four types of chain species, the initiator and monomer involved in the RAFT polymerization system, the following mass balance equations can be derived:

$$\text{for } P_r^\bullet, \quad \frac{d[P_r^\bullet]}{dt} = k_p[P_{r-1}^\bullet][M] + \frac{1}{2}k_f\sum_{s=0}^{\infty}[P_r\dot{T}P_s] - k_p[P_r^\bullet][M] - k_a[P_r^\bullet]Q_0^T - k_{td}[P_r^\bullet]Y_0 - k_{tc}[P_r^\bullet]Y_0 - k_{ct}[P_r^\bullet]Y_0^T \tag{7}$$

$$\text{for } P_r\dot{T}P_s, \quad \frac{d[P_r\dot{T}P_s]}{dt} = k_a[P_r^\bullet][TP_s] + k_a[P_s^\bullet][TP_r] - k_f[P_r\dot{T}P_s] - k_{ct}[P_r\dot{T}P_s]Y_0 \tag{8}$$

$$\text{for } TP_r, \quad \frac{d[TP_r]}{dt} = \frac{1}{2}k_f \sum_{s=0}^{\infty} [P_r\dot{T}P_s] - k_a[TP_r]Y_0 \tag{9}$$

$$\text{for } P_r, \quad \frac{d[P_r]}{dt} = k_{td}[P_r^\bullet]Y_0 + \frac{1}{2}k_{tc}\sum_{s=0}^{r}[P_s^\bullet][P_{r-s}^\bullet] - kct\sum_{s=0}^{r}[P_{r-s}^\bullet]\frac{1}{2}\sum_{t=0}^{s}[P_t\dot{T}P_{s-t}] \tag{10}$$

$$\text{for } I, \quad \frac{d[I]}{dt} = -k_d[I] \tag{11}$$

$$\text{for } M, \quad \frac{d[M]}{dt} = -k_p[M]Y_0 \tag{12}$$

Based on the method of moments and eqs. (1)–(12),[26,33] the following moment equations can be obtained:

$$\frac{dY_0}{dt} = R_1 + k_f Y_0^T - k_a Y_0 Q_0^T - k_{td}Y_0Y_0 - k_{tc}Y_0Y_0 - k_{ct}Y_0Y_0^T \tag{13}$$

$$\frac{dY_0^T}{dt} = k_a Y_0 Q_0^T - k_f Y_0^T - k_{ct}Y_0Y_0^T \tag{14}$$

$$\frac{dQ_0^T}{dt} = k_f Y_0^T - k_a Y_0 Q_0^T \tag{15}$$

$$\frac{dQ_0}{dt} = k_{td}Y_0Y_0 + \frac{1}{2}k_{tc}Y_0Y_0 + k_{ct}Y_0Y_0^T \tag{16}$$

$$\frac{dY_1}{dt} = k_p Y_0[M] + \frac{1}{2}k_f Y_1^T - k_a Y_1 Q_0^T - k_{td}Y_0Y_1 - k_{tc}Y_0Y_1 - k_{ct}Y_1Y_0^T \tag{17}$$

$$\frac{dY_1^T}{dt} = k_a Y_1 Q_0^T + k_a Y_0 Q_1^T - k_f Y_1^T - k_{ct}Y_0Y_1^T \tag{18}$$

$$\frac{dQ_1^T}{dt} = k_{td}Y_0Y_1 + k_{tc}Y_0Y_1 + k_{ct}Y_1Y_0^T + k_{ct}Y_0Y_1^T \tag{19}$$

$$\frac{dQ_1}{dt} = \frac{1}{2}k_f Y_1^T - k_a Y_0 Q_1^T \tag{20}$$

$$\frac{dY_2}{dt} = k_p Y_0[M] + 2k_p Y_1[M] + \frac{1}{2}k_f Y_{2,0}^T - k_a Y_2 Q_0^T - k_{td}Y_0Y_2 - k_{tc}Y_0Y_2 - k_{ct}Y_2Y_0^T \tag{21}$$

$$\frac{dY_2^T}{dt} = k_a Y_2 Q_0^T + 2k_a Y_1 Q_1^T + k_a Y_0 Q_2^T - k_f Y_2^T - k_{ct}Y_0Y_2^T \tag{22}$$

$$\frac{dQ_2^T}{dt} = \frac{1}{2}k_f Y_{2,0}^T - k_a Y_0 Q_2^T \tag{23}$$

$$\frac{dQ_2}{dt} = k_{td}Y_0Y_2 + k_{tc}Y_0Y_2 + k_{tc}Y_1Y_1 + k_{ct}Y_0Y_2^T + 2k_{ct}Y_1Y_1^T + k_{ct}Y_2Y_0^T \tag{24}$$

$$\frac{dY_{2,0}^T}{dt} = k_a Y_2 Q_0^T + k_a Y_0 Q_2^T - k_f Y_{2,0}^T - k_{ct}Y_0Y_{2,0}^T \tag{25}$$

In addition, the number-average chain lengths ($\bar{r}_{N,\text{tot}}$, M_n), weight-average chain lengths ($\bar{r}_{W,\text{tot}}$, M_w) and polydispersity index (PDI) for the total chain population can be described as follows[26,33]:

$$\bar{r}_{N,tot} = \frac{Y_1 + Y_1^T + Q_1 + Q_1^T}{Y_0 + Y_0^T + Q_0 + Q_0^T} \tag{26}$$

$$\bar{r}_{W,tot} = \frac{Y_2 + Y_2^T + Q_2 + Q_2^T}{Y_1 + Y_1^T + Q_1 + Q_1^T} \tag{27}$$

$$PDI = \frac{\bar{r}_{W,tot}}{\bar{r}_{N,tot}} \tag{28}$$

Correspondingly, the initial conditions are described via the following equations:

$$Y_0^T = 0 \tag{29}$$

$$Q_0^T = [CTA]_0 \tag{30}$$

$$Q_0 = 0 \tag{31}$$

$$Y_1 = 0 \tag{32}$$

$$Y_1^T = 0 \tag{33}$$

$$Q_1^T = 0 \tag{34}$$

$$Q_1 = 0 \tag{35}$$

$$Y_2 = 0 \tag{36}$$

$$Y_2^T = 0 \tag{37}$$

$$Q_2^T = 0 \tag{38}$$

$$Q_2 = 0 \tag{39}$$

$$Y_{2,0}^T = 0 \tag{40}$$

$$[I] = [I]_0 \tag{41}$$

$$[M] = [M]_0 \tag{42}$$

Accordingly, eqs. (12)–(42) consist of a set of stiff and ordinary differential equations for the RAFT process of St. The ODE23S-function provided in Matlab 6.5 software is used to solve the ordinary differential equations.

RESULTS AND DISCUSSION

Kinetic constant estimation and model verification

Relating the experimental data shown in Figures 1 and 2 with eqs. (12)–(42), the model parameters (kinetic constants) can be estimated according to the least-square method. Namely, the model parameters can be optimized through the comparison of the experimental and simulated data with an error that arrives a given minimum criterion. According to Figures 1 and 2, the experimental data include conversion and M_n, the least-square method can be described via the following eqs. (43)–(45) based on the least-square method:

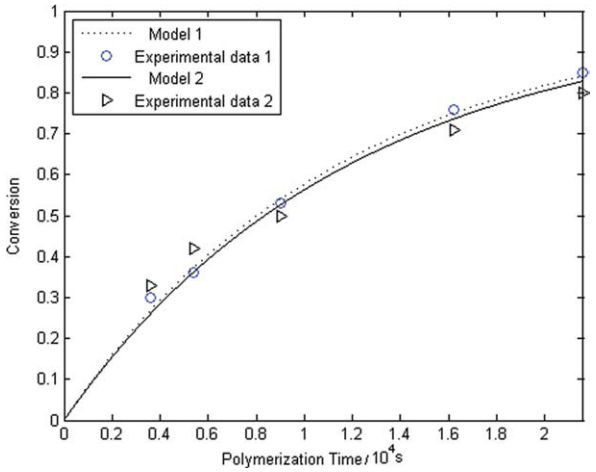

Figure 1 Comparison between experimental and simulated data of monomer conversion versus polymerization time. (Experimental data 1 stands for the RAFT polymerization with molar ratio of each component of $[M]/[T]/[I] = 100 : 1 : 1$; Experimental data 2 stands for the RAFT polymerization with molar ratio of each component of $[M]/[T]/[I] = 150 : 1 : 1$). [Color figure can be viewed in the online issue, which is available at wileyonlinelibrary.com.]

$$\text{for conversion} : \text{error1} = \sum_{i=1}^{N1} (y(\text{exp}) - y(\text{sim}))^2, \quad (43)$$

$$\text{for } M_n\text{: error2} = \sum_{i=1}^{N2} (M_n(\text{exp}) - M_n(\text{sim}))^2, \quad (44)$$

$$\text{total error} : \text{error} = \text{error1} + \text{error2}, \quad (45)$$

where, y(exp) and y(sim) are the conversions obtained via experiment and simulation, respectively, *N1* and *N2* are the total experiment numbers shown in Figures 1 and 2, respectively. The estimation process can be described briefly as follows: First, the selected initial vales for the kinetic constants and initial concentrations for all materials in the studied system are inputted. Next, the ODE23S-function provided in Matlab 6.5 software can be used to solve the ordinary differential eqs. (12)–(42). In addition, the LSQNONLIN-function provided in Matlab 6.5 software based on the least-square method is used to estimate the kinetic constants and the estimated constants are shown in Table I. Finally, eqs. (12)–(42) with the estimated constants in Table I can be used to obtain the monomer conversion, weight average molecular weight, etc.

Figures 1 and 2 illustrate that the comparisons between the experimental and the simulated results during the polymerization at two sets of feed compositions. The simulated results match experimental data well. The correlation coefficients of eqs. (12)–(42) for corresponding experimental data all exceed 0.98, which indicates that the kinetic model provide a reasonable fit for the experiment data.

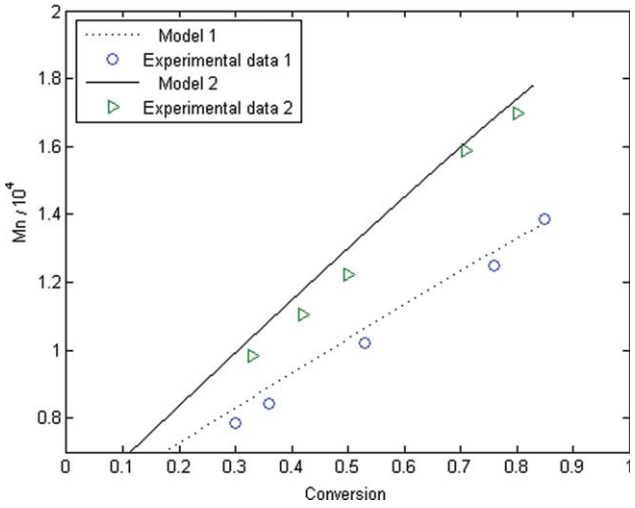

Figure 2 Comparison between experimental and simulated data of M_n depent on monomer conversion. (Polymerization conditions same as Fig. 1). [Color figure can be viewed in the online issue, which is available at wileyonlinelibrary.com.]

Model application

When the model was testified, it was used to investigate the effects of initiator concentration, chain transfer agent concentration, monomer concentration and main kinetic constants on the RAFT polymerization kinetics.

The effect of initiator concentration

Figures 3–5 illustrate the simulated effects of initiator concentration on the polymerization kinetics. It can be seen from Figures 3 and 4 that the monomer conversion increases and the number-average molecular weight of polymers keeps unchanged with the increase of initiator concentration. The above result is linked to the polymerization mechanism, namely eqs. (1)–(6). From eqs. (1) and (2), it can be found that with the increase of initiator concentration, both the monomer consuming and the number-average molecular weight of polymers increase. However, from eqs. (4)–(6), the increase of initiator concentration leads to the increase of occurrence probabilities

TABLE I
Optimal Rate Constants

k_d/s	k_p/[L/(mol s)]	k_a/[L/(mol s)]	k_f/s	k_{td}/[L/(mol s)]	k_{tc}/[L/(mol s)}	k_{ct}/[L/(mol s)]
1.0×10^{-5}	5.0×10^{3}	1.0×10^{7}	5.0×10^{4}	1.0×10^{8}	1.0×10^{8}	1.0×10^{8}

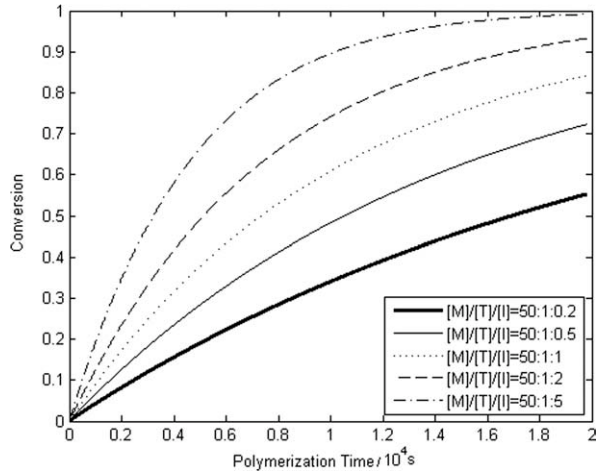

Figure 3 The simulated effect of initiator concentration on monomer conversion as a function of polymerization time.

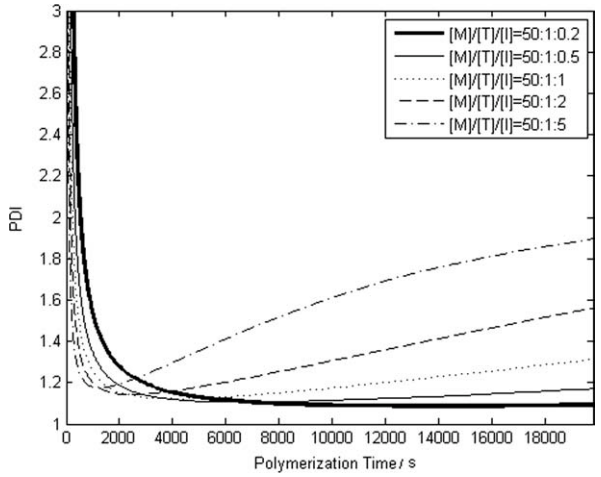

Figure 5 The simulated effect of initiator concentration on PDI as a function of polymerization time.

of the chain deactivation, which then leads to the decrease of number-average molecular weight of polymers. The final result is the nearly constant change of number-average molecular weight of polymers. Furthermore, Figure 5 shows that with the increase of initiator concentration, the polydispersity index decreases in the early period of polymerization ($t \leq 2 \times 10^3$ *s*) and increases since then ($t \leq 2 \times 10^3$ *s*). It may be due to the increase of initiator concentration leads to the increase of polymerization rate during the early period of polymerization, which turns to the increase of active-chain fraction in the polymerization system. However, during the later period, the increase of initiator concentration leads to the increase of dead-chain fraction in the polymerization system and the large difference of molecular weights between active-chain and dead-chain leads to the increase of the polymer polydispersity index. In addition, Figure 5 also shows that the narrow molecular weight distributions (PDI < 1.2) can be obtained in the RAFT polymerization process.

The effect of chain transfer agent concentration

The chain transfer agent plays a key role in the RAFT polymerization. However, there is also significant investigation as to the effect of the RAFT adduct radicals for a xanthate system used in the work.[34–36] In addition, as described in Sections "Experimental" and "Kinetic modeling of the raft process", different from a ordinary RAFT polymerization processes, the RAFT process of St reported in this work uses the PDMS-macro RAFT agent. Here, the effect of PDMS-macro RAFT agent concentration on the polymerization kinetics is simulated. The obtained simulation results are illustrated in Figures 6–8.

From Figures 6–8, one knows that the monomer conversion and the number-average molecular

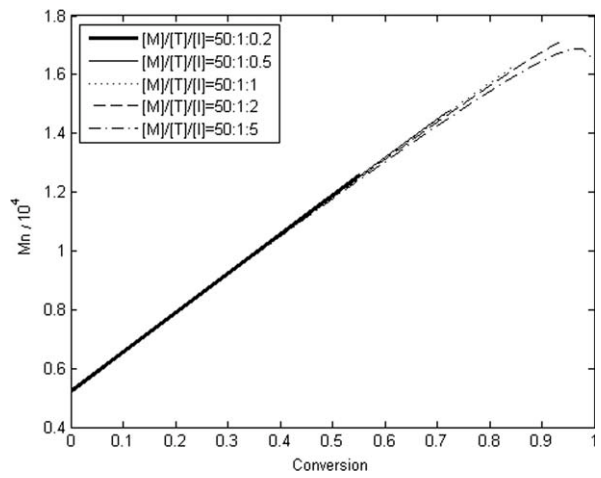

Figure 4 The simulated effect of initiator concentration on M_n as a function of monomer conversion.

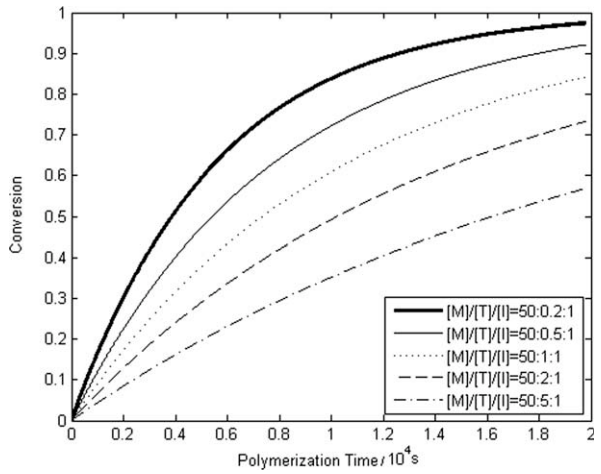

Figure 6 The simulated effect of chain transfer agent concentration on monomer conversion as a function of polymerization time.

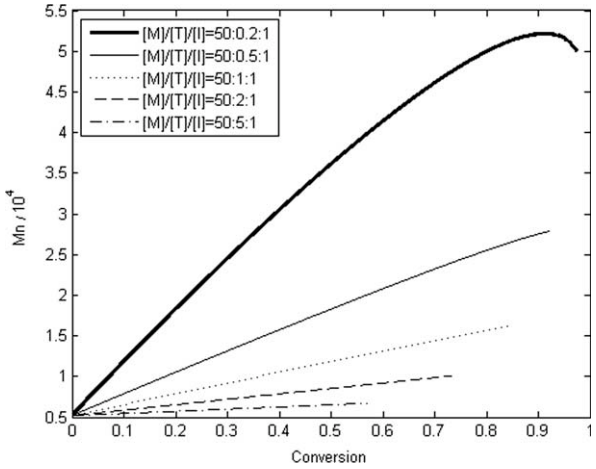

Figure 7 The simulated effect of chain transfer agent concentration on M_n as a function of monomer conversion.

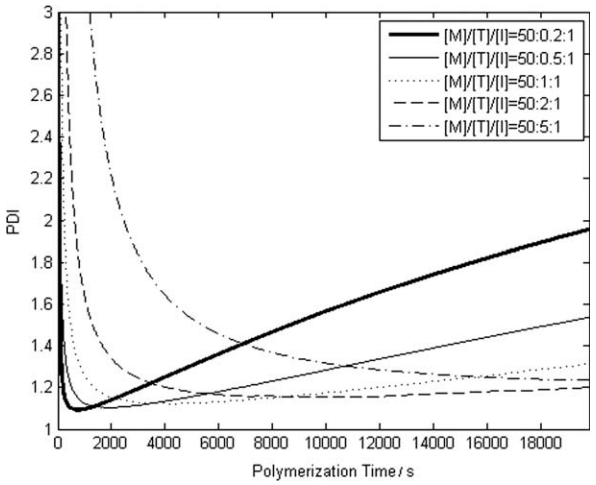

Figure 8 The simulated effect of chain transfer agent concentration on PDI as a function of polymerization time.

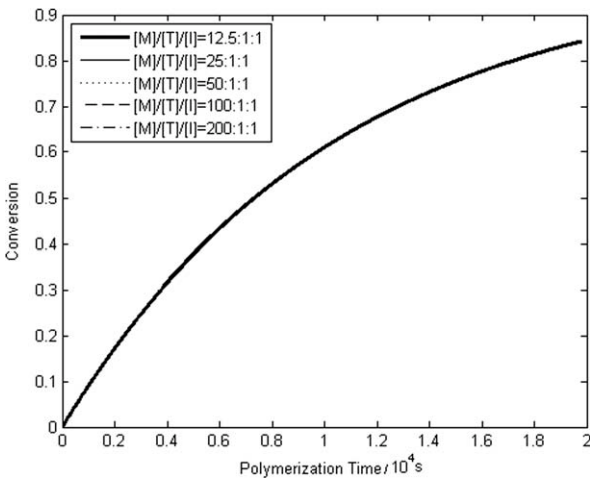

Figure 9 The simulated effect of monomer concentration on monomer conversion as a function of polymerization time.

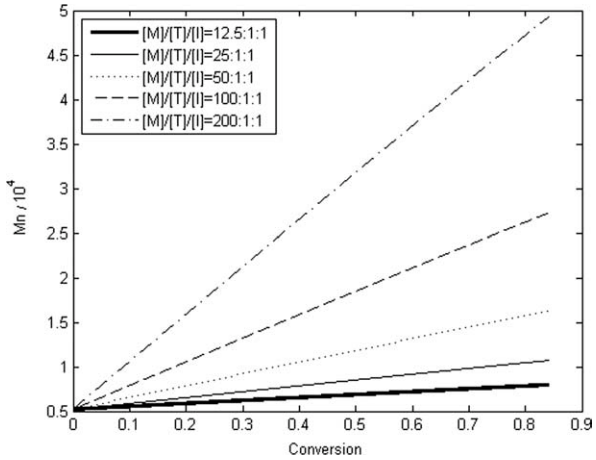

Figure 10 The simulated effect of monomer concentration on M_n as a function of monomer conversion.

weight of polymers are both decrease with the increase of chain transfer agent concentration. Different from the effect of initiator concentration described above, with the increase of chain transfer agent concentration, the polydispersity index increases in the early period of polymerization ($t \leq 5 \times 10^3$ *s*) and decreases since then ($t \geq 5 \times 10^3$ *s*) as shown in Figure 8. These results are also similar to those obtained by Wang and Zhu.[33] In addition, Wang and Zhu explained the results based on eqs. (1)–(6). Therefore, here, we do not discuss these results.

The effect of monomer concentration

In this study, the effect of monomer concentration on the polymerization kinetics is also simulated via the above model and the results are shown in Figures 9–11.

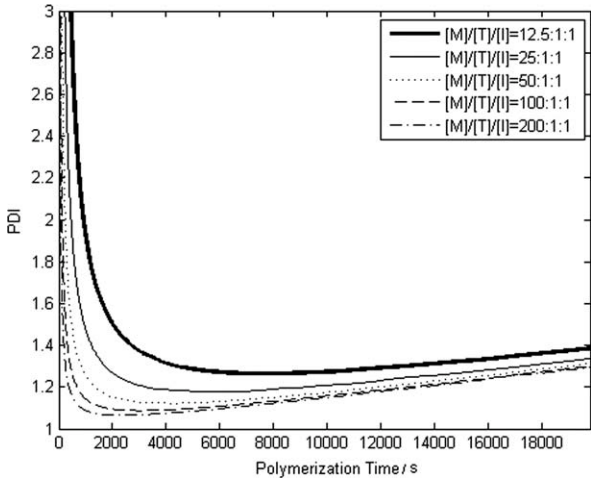

Figure 11 The simulated effect of monomer concentration on PDI as a function of polymerization time.

Figure 9 shows that the monomer conversion keeps unchanged basically with the increase of monomer concentration. As described in Figure 10, at the same monomer conversion, the number-average molecular weight of polymers increases with the increase of the monomer concentration due to high chain propagation rate. In addition, it can be seen from Figure 11 that the polydispersity index first increases and then decreases with the increase of initiator concentration. In practice, the above results can also be described via eqs. (1)–(6).

CONCLUSIONS

The PDMS-*b*-PS diblock copolymers were prepared by the RAFT polymerization using a functional PDMS-macro RAFT agent. A mathematical model for the RAFT polymerization in a batch reactor based on the method of moments was used to simulate the RAFT polymerization system. Good agreements in the polymerization kinetics were achieved for fitting the kinetic profiles with the developed model. In addition, the model was used to predict the effects of initiator concentration, chain transfer agent concentration, and monomer concentration on the RAFT polymerization kinetics.

The simulated results showed that the monomer conversion increases and the number-average molecular weight of polymers keeps unchanged basically, the polydispersity index first decreases and then increases with the increase of initiator concentration. The simulated results also showed that the monomer conversion and the number-average molecular weight of polymers are both decrease and the polydispersity index first increases and then decreases with the increase of chain transfer agent concentration. Furthermore, the simulated results indicated that the monomer conversion keeps unchanged and the number-average molecular weight of polymers increases, the polydispersity index first increases and then decreases with the increase of the monomer concentration.

The authors acknowledge the State Key Laboratory of Physical Chemistry of Solid Surfaces at Xiamen University for providing AFM facilities and assistance.

APPENDIX: DEFINITION OF MOMENTS

As described earlier, there are four types of chain species involved in the RAFT polymerization system, namely, $P_r^{\bullet}$, $P_r\dot{T}P_s$, TP_r, and P_r. Their moments are defined as follows:

$$Y_i = \sum_{r=0}^{\infty} r^i [P_r^{\bullet}] \tag{B1}$$

$$Y_i^T = \frac{1}{2}\sum_{r=0}^{\infty} r^i \sum_{s=0}^{r} [P_{r-s}\dot{T}P_s] \tag{B2}$$

$$Y_{i,j}^T = \sum_{r=0}^{\infty}\sum_{s=0}^{\infty} r^i s^j [P_r\dot{T}P_s] \tag{B3}$$

$$Q_i^T = \sum_{r=0}^{\infty} r^i [TP_r] \tag{B4}$$

$$Q_i = \sum_{r=0}^{\infty} r^i [P_r] \tag{B5}$$

References

1. Davies, W. G.; Jones, D. P. Ind Eng Chem Res 1971, 10, 168.
2. Emmanuel, P.; Jeff, T.; Cédric, E.; Patrick, L. D.; Bernard, B. Macromolecules 2006, 39, 6009.
3. Andre, M. M.; Steven, K. P.; Kebede, B. Macromolecules 2002, 35, 4238.
4. Dieng, A. C.; Lavielle, L.; Riess, G. New Polym Mater 1996, 5, 13.
5. DeSimone, J. M.; Jones, T. A.; Shaffer, K. A. Macromolecules 1996, 29, 2704.
6. DeSimone, J. M.; Betts, D. E.; Canelas, D. A. Macromolecules 1996, 29, 2818.
7. Bellas, V.; Iatrou, H.; Hadjichristidis, N. Macromolecules 2000, 33, 6993.
8. Saam, J. C.; Gordon, D. J.; Lindsey, S. Macromolecules 1970, 3, 1.
9. Bajaj, P.; Varshney, S. K. Polymer 1980, 21, 201.
10. Webster, O. W. J Polym Sci Part A: Polym Chem 2000, 38, 2855.
11. Luo, Z. H.; He, T. Y. React Funct Polym 2008, 68, 391.
12. Rosen, B. M.; Perce, V. Chem Rev 2009, 109, 5069.
13. Otsu, T.; Yoshida, M.; Tazaki, T. Macromol Rapid Commun 1982, 3, 133.
14. Hawker, C. J.; Bosman, A. W.; Harth, E. Chem Rev 2001, 101, 3661.
15. Ma, Z.; Lacroix-Desmazes, P. J Polym Sci Part A: Polym Chem 2004, 42, 2405.
16. Barner-Kowollik, C.; Davis, T. P.; Heuts, J. P.; Stenzel, M. H.; Vana, P.; Whittaker, M. J Polym Sci Part A Polym Chem 2003, 41, 365.
17. Vana, P.; Quinn, J. F.; Davis, T. P.; Barner-Kowollik, C. Aust J Chem 2002, 55, 425.
18. Zhou, D.; Zhu, X. L.; Zhu, J.; Cheng, Z. P. React Funct Polym 2009, 69, 55.
19. Mori, H.; Iwaya, H.; Endo T. React Funct Polym 2007, 67, 916.
20. Guan, C. M.; Luo, Z. H.; Tang, P. P. J Appl Polym Sci 2010, 116, 3283.
21. Soares, J. B. P. Chem Eng Sci 2001, 56, 4131.
22. Luo, Z. H.; Shi, D. P.; Zhu, Y. J Appl Polym Sci 2010, 115, 2962.
23. Wang, R.; Luo, Y.; Li, B. G.; Zhu, S. AIChE J 2007, 53, 174.
24. Sun, X.; Luo, Y.; Wang, R.; Li, B. G.; Liu, B.; Zhu, S. Macromolecules 2007, 40, 849.
25. Smulders, W. W.; Jones, C. W.; Schork, F. J. Macromolecules 2004, 37, 9345.
26. Wang, R.; Luo, Y.; Li, B. G.; Sun, X. Y.; Zhu, S. P. Macromol Theory Simul 2006, 15, 356.
27. Monteir, M. J. J Polym Sci Part A Polym Chem 2005, 43, 3189.
28. Soriano-Moro, G.; Jaramillo-Soto, G.; Guerrero-Santos, R.; Vivaldo-Lima, V. Macromol React Eng 2009, 3, 178.
29. Altarawneh, I. S.; Gomes, V. G.; Srour, M. S. Macromol React Eng 2008, 2, 58.
30. Tobita, H. Macromol React Eng 2008, 2, 371.
31. Zargar, A.; Schork, F. J. Macromol React Eng 2009, 3, 118.

32. Zhang, M.; Ray, W. H. Ind Eng Chem Res 2001, 40, 4336.
33. Wang, A. R.; Zhu, S. P. J Polym Sci Part A Polym Chem 2006, 44, 1553.
34. Junkers, T.; Theis, A.; Bubak, M.; Davis, T. P.; Stenzel, M. H.; Vana, P.; Barner-Kowollik, C. Macromolecules 2005, 38, 9497.
35. Barner-Kowollik, C.; Buback, M.; Charleux, B.; Coote, M. L.; Drache, M.; Fukuda, T.; Goto, A.; Klumperman, B.; Lowe, A. B.; Mcleary, J. B.; Moad, G.; Monteiro, M. J.; Sanderson, R. D.; Tong, M. P.; Vana, P. J Polym Sci Part A Polym Chem 2006, 44, 5809.
36. Klumperman, B.; van den Dungen, E. T. A.; Heuts, J. P. A.; Monteiro, M. J. Macromol Rapid Commun 2010, 31, 1846.